ISSN: 2583-2621

Experimental analysis of wear characteristics AISI Steel

Rajeev Ranjan
Asst. Professor,
Department of Mechanical Engineering,
Sarala Birla University Jharkhand, India
Email: raj.apx.mech@gmail.com

ABSTRACT

Wear plays a very important role in the manufacturing industry. In the present investigation the wear characteristics has been shown between AISI D3 Steel and AISI 1020 Steel. Wear effect the tool die interface and also affect the properties of work piece. The mechanical properties of AISI D3 steel against AISI 1020 steel have been analyzed. The parameters that has been discussed and considered are load and speed against time. An effort has been made to create a model in term of sliding parameters applying RSM.

KEYWORDS: pin on disk, wear rate, signal vs noise ratio, sliding parameters, anova, SEM, Taguchi methodology, orthogonal array.

INTRODUCTION

Dies are used in press working industry and during the forming process there is a sliding action of the die under a normal load condition. The parameters which play a very important role are sliding speed, Normal load and sliding distance which controls the wear behavior. All these parameters also have a significant role in the quality of products; Cost of production and rate of production hence their selection plays a vital role.

The focus of the present work is having two main objectives. The wear behavior is to be first examined for AISI D3 steel sliding against AISI 1020 steel and second is to generate wear mapping of AISI D3 steel under dry sliding condition. In order to investigate and examine the whole experimental work and result quality Taguchi methodology based on L9 orthogonal array has been selected in the present research work.

EXPERIMENTAL WORK

In order to simulate the different sliding conditions during different forming processes, experiments have been performed using a pin-on-disk tribometer. In this study, specimens (pins) of AISI D3 steel were made to slide against a rotating disk of low carbon steel (AISI 1020) under specified normal load. The independent variables that have been selected are normal load, sliding speed and sliding time. Before and after each experiment, pins were weighted. By examine the weight loss the difference in wear volume has been calculated.

ISSN: 2583-2621

Fig. 1 PIN ON DISK APPARATUS

Fig. 2 PIN ON DISK APPARATUS

ISSN: 2583-2621

Fig. 3 PIN ON DISK APPARATUS

Table 1 Technical specification of PIN ON DISK (TR-20LE-PHM-400)

Parameters	**Min**	**Max**
Pin Dimension (mm)	6	8
Disk Dimension (mm)	-	165
Wear track dia. (mm)	0	160
Speed of disk (rpm)	100	1500
Normal load (N)	10	200

FABRICATION OF PINS

In this present work, based on L9 orthogonal array-based Taguchi methodology; for the purpose of experiment total 9 pins of AISI D3 steel have been taken.

ISSN: 2583-2621

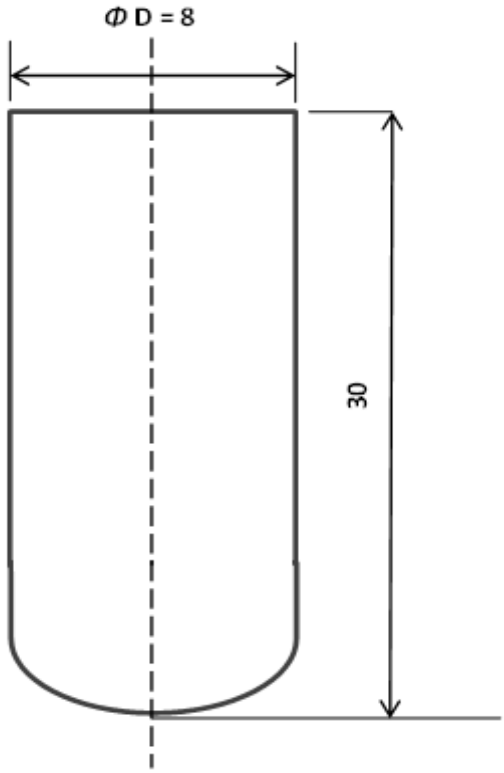

Fig. 4 Drawing, AISI D3 Steel pin (all dimensions are in mm)

Fig. 5 specimen (pin) prepared of AISI D3 steel (before wear)

ISSN: 2583-2621

Fig. 6 specimen (pin) prepared of AISI D3 steel (after wear)

The dimensions of all pins were kept 8 mm × 30 mm. The diagram of pin is given in figure 4. The figure 5 and 6 shows pins of AISI D3 steel before wear and after wear respectively.

FABRICATION OF DISK

In this present work total 2 numbers of disks of AISI 1020 steel were manufactured in order to perform all 9 experiments. Each disk is having diameter 165 mm and thickness 6 mm.

The steps involved in manufacturing of PIN are as follows:

1. Facing and Turning on lathe machine.
2. Radius forming.
3. Radius finishing.
4. Total height maintaining.

ISSN: 2583-2621

4 HOLES φ 8 EQUISPACED ON PCD $155^{\pm 0.2}$ AS SHOWN

HOLE M3 (THROUGH) AS SHOWN

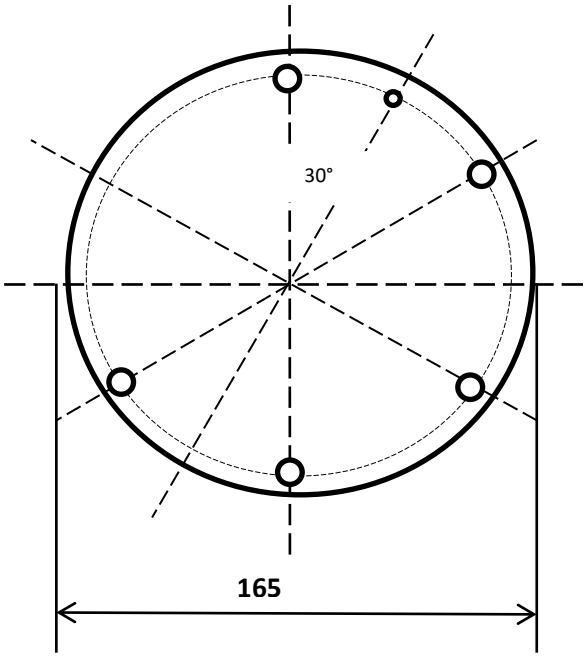

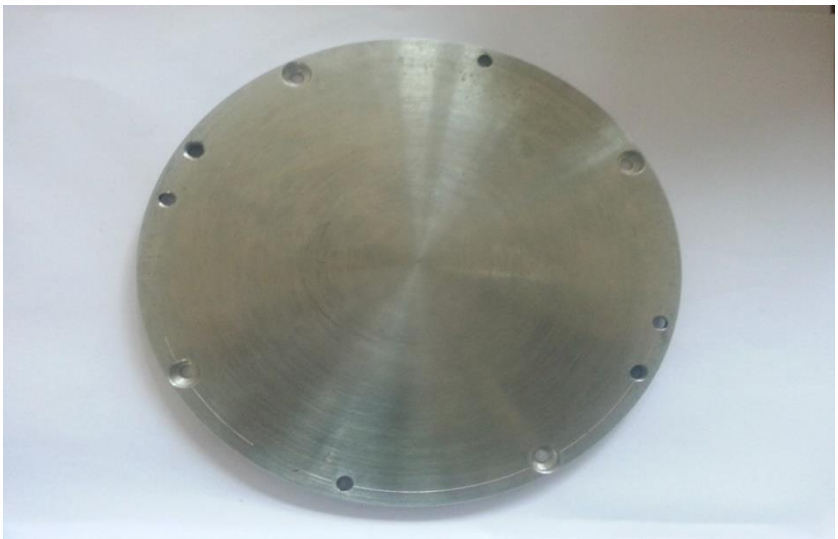

ISSN: 2583-2621

Fig. 8 AISI 1020 steel disk specimen (before wear)

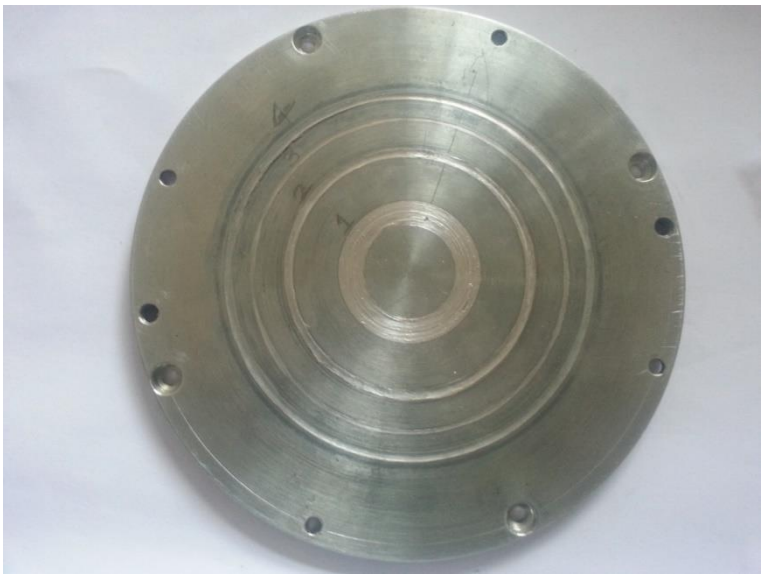

1, 2, 3 & 4 are Run numbers
Fig. 9 AISI-1020 steel specimen (after wear)

The drawing of disk is shown in fig.7. The pictorial view of disk before wear and after wear is shown in fig.8 and 9 respectively.

The steps involved in the manufacturing of disk are as followed.

1. Slicing on power hack-saw cutting machine.
2. Turning and facing on lathe machine.
3. PCD circle hole on drilling machine.
4. Hand tapping.
5. Maintaining of parallelism by surface grinding.

SIGNAL TO NOISE RATIO

A. Nominal the best

It is expressed by the equation,

$$(S/N)_{NB} = 10 \log (MSD_{NB}) = 10 \log \left[\frac{y^2}{s^2} - \left(\frac{1}{n}\right)\right] \quad (1)$$

Where y = signal factors

s = noise factors

B. Smaller the better

$$(S/N)_{LB} = -10 \log (MSD_{LB}) = -10 \log \left[(\Sigma y^2)/N\right] \quad (2)$$

C. Larger the better

$$(S/N)_{HB} = -10 \log (MSD_{HB}) = -10 \log \left[\Sigma(1/y)^2/N\right] \quad (3)$$

ISSN: 2583-2621

Table 2 Parameters and their levels according to Taguchi methodology

Parameter	Levels		
	1	2	3
Load (N)	20	30	40
Time (min.)	3	6	9
Speed (m/sec.)	1	1.5	2

Table 3 Complete design layout and experimental results

Std. order	Time(min)	Load (N)	Speed (m/sec)	Wear (gm)
1	3	20	1	0.102
2	6	20	1.5	0.0926
3	9	20	2	0.078
4	3	30	1.5	0.0286
5	6	30	2	0.0317
6	9	30	1	0.0972
7	3	40	2	0.0338
8	6	40	1	0.1078
9	9	40	1.5	0.0884

IDENTIFICATION OF MOST SIGNIFICANT WEAR PARAMETERS

Minitab 15 is used to examine 9 experiments that have been performed as per L9 orthogonal array. Significance level of $\alpha = 0.05$ is used it means the confidence level were kept 95%.

ISSN: 2583-2621

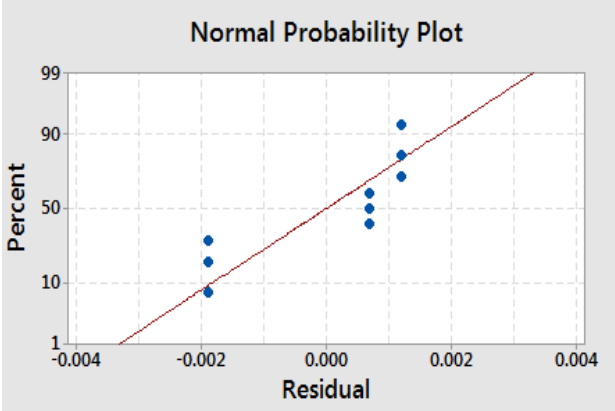

Figure 10 Residuals for mean of wear

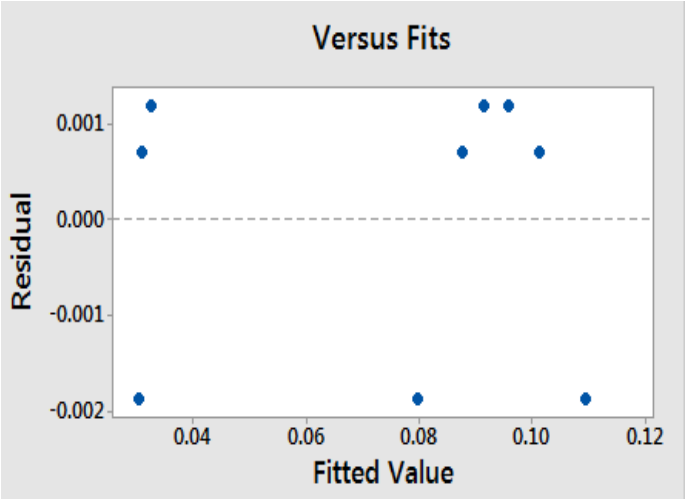

Fig. 11 Residuals v/s predicted wear

ANOVA TABLE FOR MEAN FOR WEAR

Table. 4 Resulting ANOVA table for wear

Source	Degree of freedom	Seq. sum of squares	mean square	F-Value	p-value Prob> F
Load	2	0.002258	0.001129	139	0.007
Time	2	0.001713	0.000857	105.46	0.009
Speed	2	0.00451	0.002255	277.66	0.004
residual	2	0.000016	0.000008		
Total	8	0.008497	0.001062		
R-square		99.8%	Adj. R-Square		99.2%

ISSN: 2583-2621

MINIMIZATION OF WEAR

Table 5: Response table for wear

Level					
Factors	1	2	3	Max.-Min.(Δ)	Rank
Load	0.09087	0.0525	0.07667	0.03837	2
Time	0.0548	0.07737	0.08787	0.03307	3
Speed	0.10233	0.06987	0.04783	0.0545	1

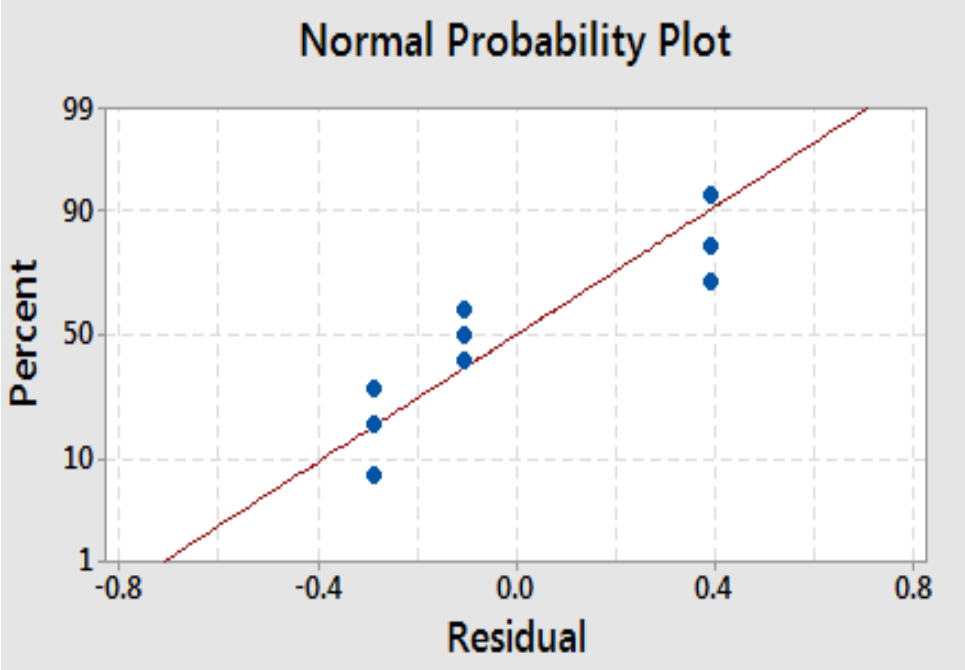

Figure.12 Residuals for S/N ratio for wear

ISSN: 2583-2621

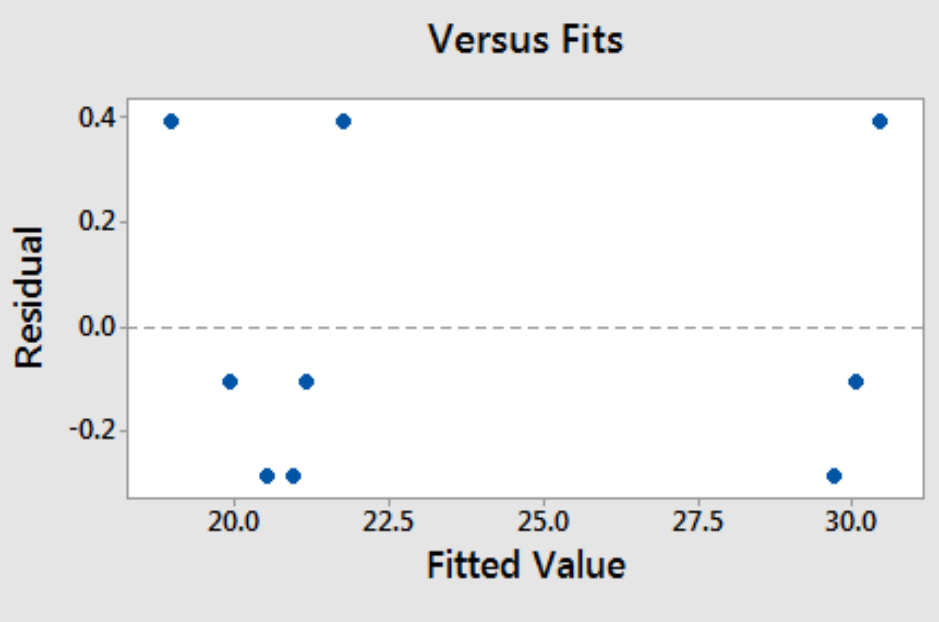

Fig. 13 Residuals v/s predicted S/N ratio for wear

ANOVA TABLE FOR S/N RATIO FOR WEAR

Table 6: ANOVA table for S/N ratio of wear

Source	Degree of freedom	Seq. sum of squares	mean square	F-Value	p-value Prob> F
Load	2	57.62	28.81	77.21	0.013
Time	2	46.909	23.4545	62.86	0.016
Speed	2	82.669	41.3345	110.78	0.009
residual	2	0.746	0.373		
Total	8	187.944			
R-square		99.6%	Adj. R-Square		98.4%

ISSN: 2583-2621

MINIMIZATION OF WEAR USING S/N RATIO

Table 7: S/N ratio (minimum is best) table for wear

	Level				
Factors	1	2	3	Max.-Min.(Δ)	Rank
Load	20.88	27.03	23.28	6.15	2
Time	26.71	23.33	21.16	5.55	3
Speed	19.81	24.2	27.19	7.38	1

The maximum of all these values reflect the most effective factor. Out of these values it has been observed that speed plays a very significant role after that load and at last time. Same result has been obtained as obtained from mean of wear. SEM observations also reflect different types of wears.

EFFECT OF NORMAL LOAD ON WEIGHT LOSS

Speed= 1.5m/s and Time= 6 minute

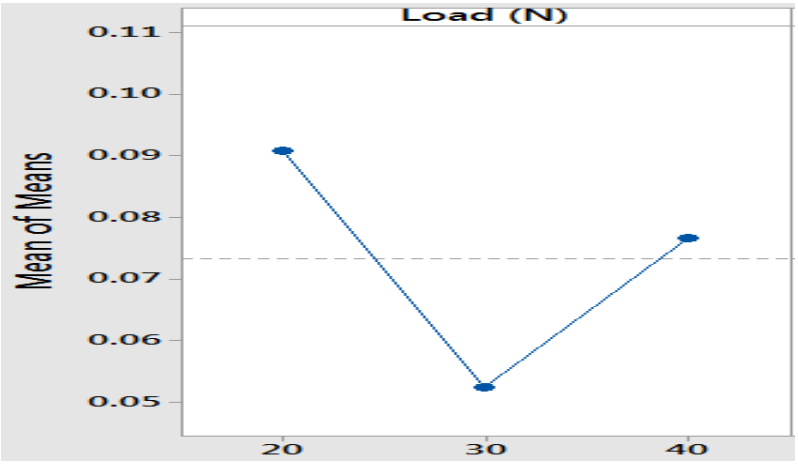

Figure 14 Effect of load on wear

ISSN: 2583-2621

EFFECT OF SLIDING SPEED ON WEIGHT LOSS

Load= 30 N and Time= 6 minute

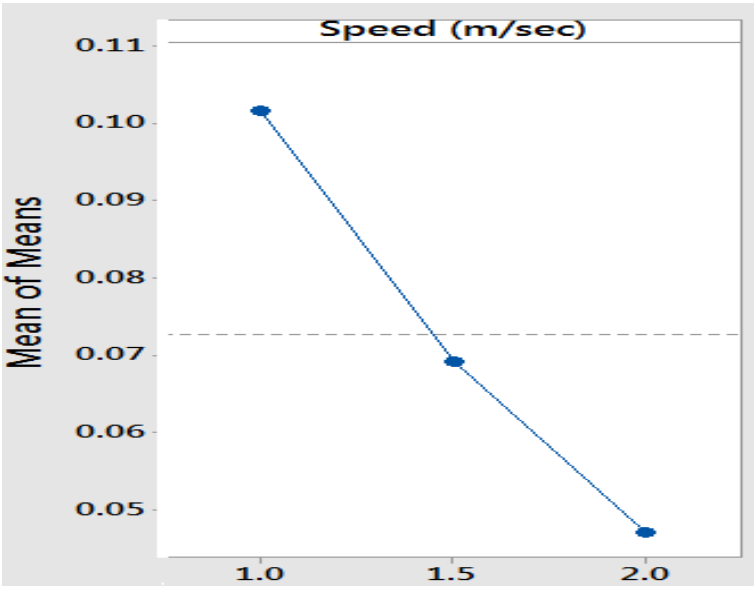

Figure 15 Effect of sliding speed on wear

EFFECT OF SLIDING TIME ON WEIGHT LOSS

Speed= 1.5m/s and Load= 30 N

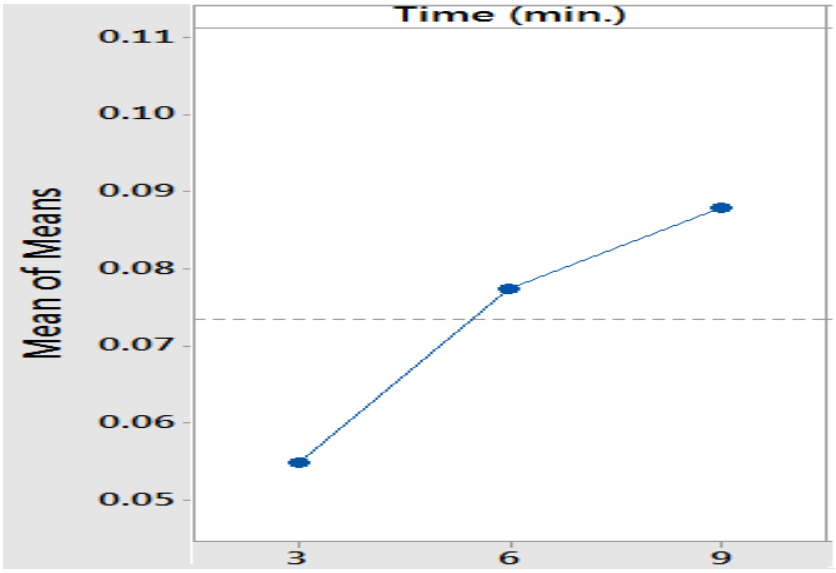

Figure 16 Effect of time on wear

ISSN: 2583-2621

SEM OBSERVATIONS

According to the SEM observations, when load was 20N, speed was 1 m/s and time was 9 min, the worn surface of AISID3 steel pin appears relatively rough as shown in fig 17**.** The micrograph qualitatively correlates well with the weight loss measurements. This micrograph clearly demonstrates the signs of abrasion wear along with some patches of ploughing but abrasion wear is the dominating wear at given conditions. When load was 30N, the wear exposed surface no longer appears clean as shown in fig 18. This micrograph clearly depicts that as the load was increased from the previous level, the surface visually appears rougher. There are the signs of abrasion wear along with the indications of adhesion wear. When load was 40 N and speed was 1.5 m/s and time was 6 min, the worn-out surface is shown in fig 19. Hence this micrograph clearly depicts the effect of load. When load was increased from a certain level, like in this case load was above 30 N, the transition of wear mechanism took place and spalling and ploughing of D3 steel surface became the dominating wear mechanism as the signs of abrasion were disappear and surface becomes more and more rough.

SEM micrographs of the worn-out pin surface at three different speeds of 1 m/s, 2 m/s and 1.5 m/s are shown in fig. 17, 18 & fig. 19 respectively. These micrographs can be easily correlated with the weight loss measurements.

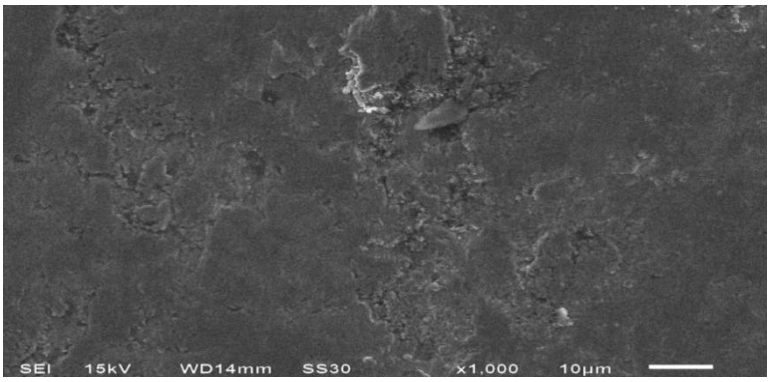

Fig. 17, SEM image shows worn surfaces of AISI D2 steel pin at load 20, speed 1 m/s, time 9 min

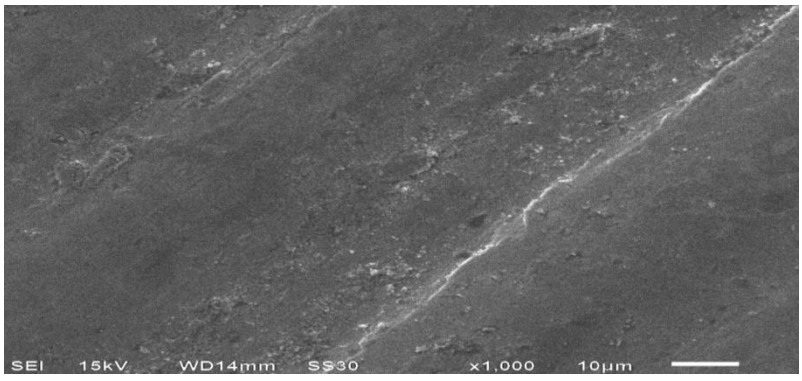

Fig. 18, SEM image of worn surface of AISI D2 steel pin at load30N, speed 2 m/s, time 3 min

ISSN: 2583-2621

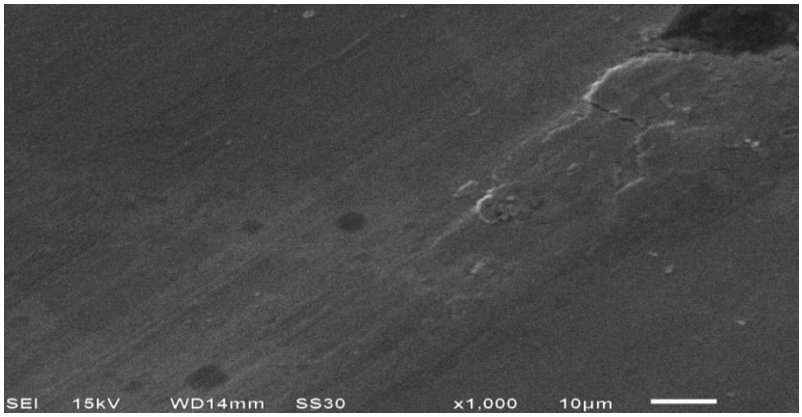

Fig. 19, SEM image of worn surface of AISI D3 steel pin at load 40 N, speed 1.5 m/s, time 6 min

RESULT AND DISCUSSION:

The following are by far the most noteworthy insights drawn from this research:

1. All the three independent parameters i.e load, speed and time give impression of being the significant sliding parameter.
2. By SEM inspection without doubt it can be seen that the effect of the speed is found to be most influential factor followed by time and load.
3. The wear amount or weight loss increases with increasing sliding time.
4. The wear amount or weight loss decreases with increasing sliding speed.

REFERENCES

1. A. Alsaran, A. Celik, M. Karakan (2005). Structural, mechanical and tribological properties of duplex-treated AISI 5140 steel, *Materials Characterization*, Vol. 54, pp. 85-92.
2. A. Alsaran, A. Celik, C. Celik, I. Efeoglu (2004). Optimization of coating parameters for duplex treated AISI 5140 steel, *Material Science and Engineering*, Vol. 371, pp. 141-148.
3. A.S. Galakhar, J.D. Gates, W.J. Daniel, P.A. Meehan (2011). Adhesive tool wear in the cold roll forming process, *Wear*, Vol. 271, pp. 2728-2745.
4. A. Toro, C. Viafara, M. Castro, J. Velez (2005). Unlubricated sliding wear of pearlitic and bainitic steels, *Wear*, Vol. 259, pp. 405-411.
5. B. Podgornik, J. Vizintin, H. Ronkainen, K. Holmberg (2000). Friction and wear properties of DLC-coated plasma nitrided steel in unidirectional and reciprocating sliding, *Thin Solid Films*, Vol. 377-378, pp. 254-260.
6. B. Rajasekaran, G. Mauer, R. Vaben, A. Rottger, S. Weber, W. Theisen (2010). Thick tool steel coatings using HVOF spraying for wear resistance applications, *Surface & Coatings Technology*, Vol. 205, pp. 2449-2454.

7. B.S. Yilbas, S.M. Nizam (2000). Wear behavior of TiN coated AISI H11 AISI M7 twist drills prior to plasma nitriding, *Journal of Materials Processing Technology*, Vol. 105, pp. 352-358.
8. C. Boher, S. Roux, L. Penazzi, C. Dessain (2012). Experimental investigation of the tribologicalbehavior and wear mechanisms of tool steel grades in hot stamping of a high-strength boron steel, *Wear*, Vol. 294-295, pp. 286-295.
9. C. Spero, D.J. Hargreaves, R.K. Kirkcaldie, H.J. Flitt (1991). Review of test methods for abrasive wear in ore grinding, *Wear*, Vol. 146, pp. 389-408.
10. C. Lee, A. Sanders, N. Tikekar, K.S. Ravi (2008). Tribology of titanium boride-coated titanium balls against alumina ceramic: wear, friction and micromechanisms, *Wear*, Vol. 265, pp. 375-376.
11. D.A. Rigney (1994). The roles of hardness in the sliding behavior of materials, *Wear*, Vol. 175, pp. 63-69.
12. D. Camino, A.H.S. Jones, D. Mercs, D.G. Teer (1999). High performance sputtered carbon coatings for wear resistant applications, *Vacuum*, Vol. 52, pp. 125-131.
13. D. Das, A.K. Dutta, K.K. Ray (2009). Optimization of the duration of cryogenic processing to maximize wear resistance of AISI D2 steel, *Cryogenics*, Vol. 49, pp. 176-184.
14. D. Das, A.K. Dutta, K.K. Ray (2010). Sub-zero treatments of AISI D2 steel: part II. Wear behavior, *Material Science and Engineering*, Vol. 527, pp. 2194-2206.
15. E. Schedin (1994). Galling mechanisms in sheet metal forming operations, *Wear*, Vol. 179, pp. 123-128.
16. E. Vera, G.K. Wolf (1999). Optimization of TiN-IBAD coatings for wear reduction and corrosion protection, *Nuclear Instruments and Methods in Physics Research*, Vol. 148, pp. 917-924.
17. F. Klocke, T. Mabmann, K. Gerschwiler (2005). Combination of PVD tool coatings and biodegradable lubricants in metal forming and machining, *Wear*, Vol. 259, pp. 1197-1206.
18. G.B. Wang (1997). Wear mechanisms in vanadium carbide coated steel, *Wear*, Vol. 212, pp. 25-32.
19. G. Cueva, A. Sinatora, W.L. Guesser, A.P. Tschiptschin (2003). Wear resistance of cast irons used in brake disc rotors, *Wear*, Vol. 255, pp. 1256-1260.
20. H. So (1995). The mechanism of oxidational wear, *Wear*, Vol. 184, pp. 161-167.
21. H. So (1996). Characteristics of wear results tested by pin-on-disc at moderate to high speeds, *Tribology International*, Vol. 29, pp. 415-423.
22. H. So, D.S. Yu, C.Y. Chuang (2002). Formation and wear mechanism of tribo – oxides and the regime of oxidational wear of steel, *Wear*, Vol. 253, pp. 1004-1015.
23. H. Sui, H. Pohl, U. Schomburg, G. Upper, S. Heine (1999). Wear and friction of PTFE seals, *Wear*, Vol. 224, pp. 175-182.
24. I.V. Kragelsky, A.I. Zolotar, A.O. Sheiwekhman (1985). Theory of material wear by solid particle impact – a review, *Tribology International*, Vol. 18, pp. 3-11.
25. J.D. Bressan, R. Hesse, E.M. Silva Jr. (2001). Abrasive wear behavior of high speed steel and hard metal coated with TiAlN and TiCN, *Wear*, Vol. 250, pp. 551-568.